

## Observation of interference in transitions due to local geometric phases

D. Bouwmeester, G. P. Karman, C. A. Schrama, and J. P. Woerdman  
*Huygens Laboratory, University of Leiden, P.O. Box 9504, 2300 RA Leiden, The Netherlands*  
 (Received 18 October 1995)

We present an optical implementation of a twisted Landau-Zener model for which local aspects of the geometric phase strongly influence the transition amplitude. The transition amplitude is influenced by an interference effect caused by the interplay between geometric and dynamic phases.

PACS number(s): 32.80.Bx, 03.65.Bz, 34.10.+x

### I. INTRODUCTION

A geometric phase is, by definition, the phase change of a state function due to the curvature of a specific path followed in parameter space. Usually the geometric phase is considered for a closed path; therefore it is often expressed as a closed circuit integral in parameter space [1,2]. Such an expression is explicitly time independent and brings out the global properties of path followed in the parameter space. The interest in this paper is, however, not in such global aspects of the geometric phase but rather in its local aspects. These local aspects, i.e., the contribution of geometric phase to the state function that arises for an open path, may strongly influence transition phenomena as pointed out by Berry [3] and others [4,5].

As an example, consider a two-level system for which the two adiabatic eigenstates perform an avoided crossing. Assume that, due to the particular curvature of the corresponding path in parameter space, the adiabatic eigenstates acquire an opposite geometric phase which changes in time. Since a time-dependent phase corresponds to an energy shift, the energy difference between the two adiabatic eigenstates is effectively changed. According to familiar dynamical Landau-Zener arguments this results in a change in the transition amplitude.

In the original paper by Berry [3] this change is mathematically described in the adiabatic limit by multiplying the dynamical transition amplitude by a so-called geometric amplitude factor. In the adiabatic limit transitions are exponentially weak and the geometric amplitude factor is of the order unity. Experimental results in this limit have been presented in Ref. [6]. Recently it was shown that the derivation given by Berry is unnecessarily restrictive [4,5]. In the general case the effect of the geometric phase on the transition amplitude can no longer be described as a simple multiplicative factor but manifests itself in an intertwined way with the dynamical evolution. In this paper we report on the experimental observation of the very pronounced features in the transition amplitude induced in this general case by the geometric phase.

### II. TWISTED LANDAU-ZENER MODEL

We consider an optical implementation of the *twisted* Landau-Zener (LZ) model [3], which is characterized by the following Hamiltonian,

$$H_{\text{twist}} = \begin{pmatrix} \alpha t & \Delta \exp\{-i\phi(t)\} \\ \Delta \exp\{+i\phi(t)\} & -\alpha t \end{pmatrix}. \quad (1)$$

We will refer to  $\phi(t)$  as the twist function. Note that the twisted LZ model is not merely an academic construction for illustrating geometric influences on transition amplitudes; in fact it is the natural generalization of the highly valuable conventional Landau-Zener model [ $\phi(t)=0$ ]. The inclusion of the twist function in the LZ model does not change the adiabatic energy levels  $E_{\pm}(t)$ ; however, it does induce curvature in the path followed in parameter space. For two-level systems it is convenient to introduce as coordinates of the parameter space  $X(t), Y(t), Z(t)$ , defined through

$$H(t) = \begin{pmatrix} Z(t) & X(t) - iY(t) \\ X(t) + iY(t) & -Z(t) \end{pmatrix}. \quad (2)$$

The path followed in parameter space by the conventional LZ model is a straight line, indicated in Fig. 1(a) by the dotted line. In this case no geometric effects can occur. For the twisted LZ model the path is winding and unwinding in parameter space as shown in Fig. 1(a) by the solid curve [for  $\phi(t)=\beta t^2$ ]. The winding motion gives rise to opposite geometric-phase contributions  $\gamma_{\pm}$  to the two adiabatic eigenstates  $|+\rangle$  and  $|-\rangle$  of  $H_{\text{twist}}$ . Expressions for the geometric phases are obtained using the Schrödinger equation and the adiabatic approximation [1]. In the two-level case defined by  $H_{\text{twist}}$  they are given by

$$\gamma_{\pm}(t) = \frac{1}{\hbar} \int_0^t \left\langle \pm \left| \frac{d}{dt'} \right| \pm \right\rangle dt' = \frac{1}{2} \int_0^t \dot{\phi}(t') \frac{\alpha t'}{E_{\pm}} dt', \quad (3)$$

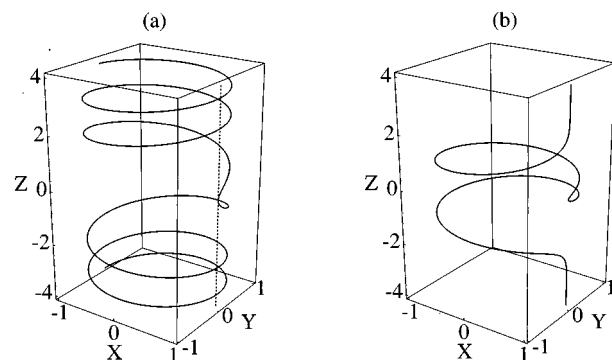


FIG. 1. Hamiltonian curves for (a) the conventional Landau-Zener model (dotted line), and for the twisted Landau-Zener model in the case of  $\phi(t)=\beta t^2$  (solid curve); (b) the Gaussian twisted Landau-Zener model.

where the overdot denotes a derivative with respect to time.

At this point we should mention that although this paper deals with classical optical experiments the occurrence of  $\hbar$  in the formulas is not disturbing. We merely choose to adopt the familiar quantum-mechanical two-level description in terms of energy levels instead of frequency levels. Using the well-known relation  $E = \hbar \omega$  allows for a simple transformation of the quantum-mechanical to the classical formulation.

By making a time-dependent transformation to a frame comoving with  $\phi(t)$ , hereafter referred to as the winding frame, the geometric phases can be expressed as dynamical phases [3]. After the transformation the Hamiltonian has the same form as the conventional LZ model and the geometric effects now manifest themselves in the adiabatic energy levels,

$$E'_{\pm} = \pm \sqrt{(Z - \frac{1}{2}\hbar\dot{\phi})^2 + X^2 + Y^2}. \quad (4)$$

Primed quantities refer to quantities in the winding frame. To describe the influence of  $\phi(t)$  on the transition amplitude we employ the Dykhne-Davis-Pechukas (DDP) method [7] in the winding frame. This method is, just like the derivation of the geometric phase, based on the adiabatic approximation and is therefore suited to incorporate effects of geometric origin. According to the adiabatic assumption transitions between adiabatic energy levels can only occur at positions where the adiabatic energy levels are degenerate. For avoided crossing models there do not exist such positions for real values of time. However, the essence of the DDP method is that by continuation of adiabatic following into the complex time plane there do exist such degeneracies at points  $t_c$ . These points come in conjugate pairs, and are the branch points of the square-root expression for  $E'_{\pm}$ .

For the real symmetric Hamiltonian in the winding frame the adiabatic “evolution” of  $|\Psi'(t)\rangle$  from  $t=0$ , where we assume that  $|\Psi'(0)\rangle = |+\rangle$ , to the branch point  $t=t_c$ , reads

$$|\Psi'(t_c)\rangle = \exp\left\{-\frac{i}{\hbar} \int_0^{t_c} E'_+(t) dt\right\} |+\rangle. \quad (5)$$

Since the time is complex valued, the exponent in Eq. (5) no longer describes a pure phase factor. Instead it also describes damping if the branch point is chosen in the lower half of the time plane. Subsequent integration along an infinitesimal small circle around the square-root branch point  $t_c$  provides a minus sign, which is the same as interchanging the labels of the adiabatic eigenstates at  $t_c$ . Note that this minus sign accomplishes the actual transition. It can also be interpreted as a geometric phase of  $\pm \pi$  [1]. Integration along the return path to the real time axis gives the same exponential factor as in Eq. (5). The total transition probability  $P$  is now given by  $\exp\{-\Gamma\}$ , with

$$\Gamma = -\frac{4}{\hbar} \text{Im} \int_0^{t_c} E'_+(t) dt. \quad (6)$$

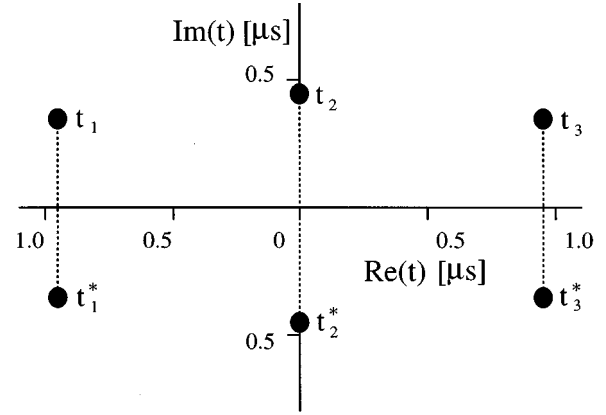


FIG. 2. The dots indicate the three pairs of branch points which dominate the transition phenomena for the Gaussian twisted Landau-Zener model ( $\alpha=0.44$  MHz/ $\mu$ s,  $\Delta=0.33$  MHz,  $a=1$   $\mu$ s, and  $\mu=5.4$  rad). The asterisk denotes the complex conjugate.

### III. INTERFERENCES

Our key point is that Eq. (4) has more than one pair of branch points for twist functions which fulfill the physical requirement of possessing a finite value at  $t \rightarrow \pm \infty$  [5]. In this situation there are several ways in which the initial state  $|+\rangle$  can end up in the final state  $|-\rangle$ , hence interference terms will arise in the expression for the total transition probability  $P$ . Only branch points for which the corresponding  $\Gamma$  [see Eq. (6)] is relatively small will significantly contribute to  $P$  [8]. We introduce for our experiments the following “physical” twist function

$$\phi(t) = \mu(1 - \exp\{-t/a\}^2), \quad (7)$$

with  $\mu$  and  $a$  real valued. We will refer to this model as the Gaussian twisted Landau-Zener model. The path followed in parameter space is drawn in Fig. 1(b). In the parameter region relevant for our experiment the transition phenomena are dominated by three pairs of branch points as shown in Fig. 2.

The transition probability is expected to show interference phenomena similar to the transition probability for a sequence of three avoided crossings. An analytical expression for the transition probability, using the DDP method in the primed frame and taking into account the three nearest pairs of branch points shown in Fig. 2, is obtained as follows. For an incoming wave function  $|\Psi_i\rangle$ , the outgoing wave function  $|\Psi_f\rangle$ , i.e., the wave function after passing the sequence of crossings, is determined by

$$|\Psi_f\rangle = U(t_3)U(t_2 \rightarrow t_3)U(t_2)U(t_1 \rightarrow t_2)U(t_1)|\Psi_i\rangle, \quad (8)$$

where  $U(t_1 \rightarrow t_2)$  and  $U(t_2 \rightarrow t_3)$  represent free propagation along the real time axis in between the positions of the branch points, and  $U(t_i)$  ( $i=1,2,3$ ) represent the passage of the branch points. As expressions for  $U(t_1 \rightarrow t_2)$ , and similarly for  $U(t_2 \rightarrow t_3)$ , we find

$$U(t_1 \rightarrow t_2) = \begin{pmatrix} \exp\left\{-\frac{i}{\hbar} \int_{\text{Re}[t_1]}^{\text{Re}[t_2]} E'_+ dt\right\} & 0 \\ 0 & -\exp\left\{-\frac{i}{\hbar} \int_{\text{Re}[t_1]}^{\text{Re}[t_2]} E'_+ dt\right\} \end{pmatrix}, \quad (9)$$

and for  $U(t_i)$

$$U(t_i) = \begin{pmatrix} \left[1 - \left|\exp\left\{-\frac{2i}{\hbar} \int_{\text{Re}[t_i]}^{t_i^*} E'_+ dt\right\}\right|^2\right]^{1/2} & \exp\left\{\frac{2i}{\hbar} \int_{\text{Re}[t_i]}^{t_i} E'_+ dt\right\} \\ \exp\left\{-\frac{2i}{\hbar} \int_{\text{Re}[t_i]}^{t_i^*} E'_+ dt\right\} & e^{i\psi} \left[1 - \left|\exp\left\{\frac{2i}{\hbar} \int_{\text{Re}[t_i]}^{t_i} E'_+ dt\right\}\right|^2\right]^{1/2} \end{pmatrix}, \quad (10)$$

where

$$E'_+ = \sqrt{\left(\alpha t - \frac{1}{2} \hbar \dot{\phi}\right)^2 + \Delta^2}, \quad (11)$$

with  $\phi$  given in Eq. (7). The off-diagonal elements of  $U(t_i)$  are obtained from Eq. (6). The diagonal elements are calculated by noting that when the probability for making a transition is  $P$ , then the probability for not making a transition is  $1 - P$ . Hence the amplitude for not making a transition is a phase factor times  $\sqrt{1 - P}$ . A point of concern is that  $U(t)$  should be unitary. This can be achieved by an appropriate choice of  $\psi$ . The choice of  $e^{i\psi} = -1$  fulfills this requirement.

The analytical results for the final transition probability  $P$  for different values for  $\Lambda$  are plotted in Fig. 3 (circles connected by the solid curve 1). For comparison we also plotted the conventional LZ curve (dotted curve 2). The most significant difference between the two curves is the presence of a local minimum in  $P$  for the twisted Landau-Zener curve, which is a clear indication of the presence of interferences.

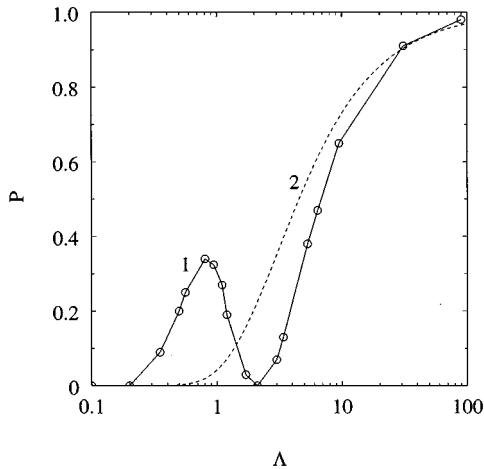


FIG. 3. The circles connected by curve 1 are the analytical results for the final transition probability  $P$  for different values for  $\Lambda$ , in the case of the Gaussian twisted Landau-Zener model. Curve 2 is the conventional Landau-Zener curve.

#### IV. EXPERIMENTAL DEMONSTRATION

For our experiments we used an optical two-level system which is schematically shown in Fig. 4. The mapping of the optical two-level system to a quantum-mechanical two-level system has been discussed in previous publications [9]. Here we will present only a brief outline of the mapping. The two optical levels are formed by two orthogonal polarization states of a single longitudinal mode of an optical ring cavity. The instantaneous polarization eigenstates correspond to the two adiabatic energy eigenstates of the general two-level Hamiltonian given by Eq. (2). The two eigenstates are determined by three birefringent elements in the form of electro-optic modulators (EOM's), placed inside the optical cavity. To calculate these eigenstates the Jones matrix formalism is used [10]. The birefringences of the three EOM's form, after a simple linear transformation, the three coordinates  $X$ ,  $Y$ , and  $Z$  of the parameter space. They can be controlled by applying electric voltages to the EOM's so that any path in

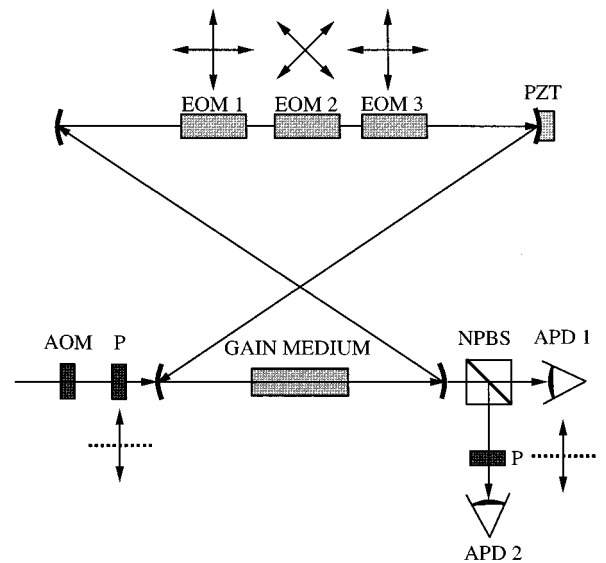


FIG. 4. Schematic drawing of the optical part of the setup. The acronyms used are AOM for acousto-optic modulator,  $P$  for polarizer, EOM for electro-optic modulator, PZT for piezoelectric element, NPBS for nonpolarizing beam splitter, and APD for avalanche photodiode.

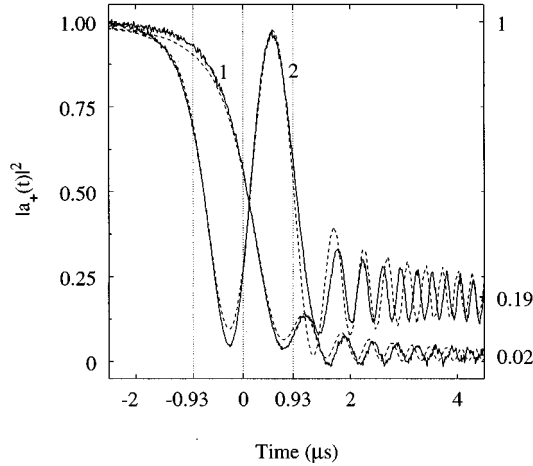


FIG. 5. Experimental results: curve 1 shows the time trace of  $|a_+(t)|^2$  for the conventional Landau-Zener model,  $\alpha=0.44$  MHz  $\mu\text{s}^{-1}$ ,  $\Delta=0.33$  MHz; curve 2 shows the time trace for the Gaussian twisted Landau-Zener model for the same values for  $\alpha$  and  $\delta$  and for  $a=1$   $\mu\text{s}$ ,  $\mu=5.4$  rad. The dotted curves show the corresponding traces obtained by numerical simulations. The vertical dotted lines indicate the time positions that correspond to the real parts of the branch points shown in Fig. 2.

the parameter space of the general two-level model can be traced experimentally.

The initial state of the optical two-level system is prepared by a single-frequency He-Ne injection laser with a well-defined polarization. Using a piezoelectric-transducer-mounted mirror (PZT), the ring cavity is tuned into resonance with the injection light. At a certain intracavity intensity the injection light is switched off by an acousto-optic modulator (AOM), and the actual experiment starts. Within the cavity decay time the path in parameter space shown in Fig. 1(b) is implemented by the time-dependent voltages applied to the EOM's. We designed a polarization-independent He-Ne light amplifier to enhance the cavity decay time to approximately 10  $\mu\text{s}$ , which is sufficiently long to realize such an experiment. The dynamics of the intracavity field is measured by analyzing the polarization of light that leaks out through one of the cavity mirrors.

Two typical experimental results are shown in Fig. 5. The horizontal axis is the time axis where  $t=0$  is chosen to coincide with  $t=0$  in Fig. 2. Plotted on the vertical axis is the normalized intensity of the + polarization,  $|a_+(t)|^2$ . The + polarization coincides with the injection polarization. We analyze the system in the diabatic, i.e., the uncoupled, basis. Since the diabatic and adiabatic bases coincide far away from the crossing region we can determine the transition probability  $P$  between the adiabatic states from the diabatic population on the right-hand side of Fig. 5.

Curve 1 of Fig. 5 shows the experimental results for the conventional LZ model in the near adiabatic region ( $P=0.02$ ). Note that the oscillating structure after the avoided crossing at  $t=0$  indicates that in the crossing region the adiabatic eigenstates of the system are superpositions of the + and - polarization.

Curve 2 is the time trace of  $|a_+(t)|^2$  for the Gaussian twisted LZ model corresponding to the branch points plotted in Fig. 2. It clearly illustrates the influence of the three pairs

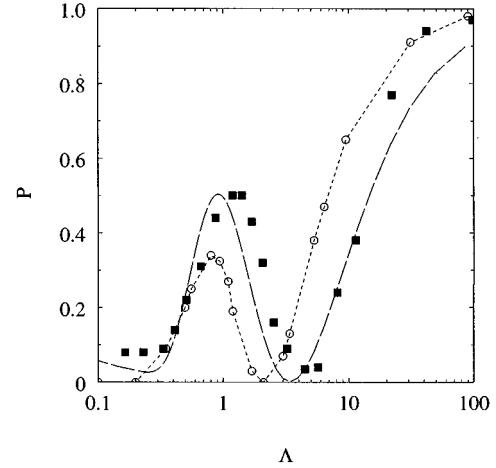


FIG. 6. The square points are the experimentally obtained values for the final transition amplitude  $P$  as function of  $\Lambda$ . Experimentally  $\Lambda$  has been changed by varying  $\Delta$ , while  $\alpha=0.49$  MHz  $\mu\text{s}^{-1}$ ,  $a=0.72$   $\mu\text{s}$ , and  $\mu=3.0$  rad were kept constant. The dashed curve represents the corresponding numerical results. The circles connected by the dotted curve are the corresponding analytical results as obtained in Sec. III under the approximation that only the three nearest pairs of branch points to the real time axis are taken into account.

of branch points of which the real parts are indicated by the dotted vertical lines at  $t=0$  and  $t=\pm 0.93$   $\mu\text{s}$ . The values for  $\alpha$  and  $\Delta$  are the same as for curve 1. Therefore, all differences between the time traces 1 and 2 are exclusively the consequence of the twist function. The dotted curves show the numerically obtained traces which are in good agreement with the experimental traces.

As explained in Sec. III, the occurrence of a sequence of three avoided crossings is expected to give rise to interference phenomena in the transition probability. To measure these interferences we performed a series of Gaussian twisted LZ experiments for different values for  $\Delta$ . The experimental data for the final transition probability  $P$  between the adiabatic energy levels is plotted as function of the adiabaticity parameter  $\Lambda \equiv \alpha/2\pi\Delta^2$  in Fig. 6. There is a good agreement between our experimental data (square points) and the numerical results (dashed curve). There is also rough agreement between our experimental data and the approximated analytical results (circles connected by dotted curve) obtained in Sec. III. In particular, the interference phenomenon is clearly illustrated by the minimum at  $\Lambda \approx 3$ .

## V. CONCLUSIONS

We have experimentally demonstrated that a single avoided crossing can behave as a sequence of avoided crossings due to the presence of geometric phases. Interference between the successive crossings strongly influences the transition probability. In particular, we introduced the Gaussian twisted Landau-Zener model and compared the transition properties to those of the conventional Landau-Zener model.

We supported our experimental results by numerical simulations and by analytical calculations based on the DDP method. The numerical results are in good agreement with the experimental results whereas the analytical results show

only a qualitative agreement. The reason that only rough agreement is obtained in the analytical case is probably due to the fact that we took only the three nearest pairs of branch points in the primed frame into account, and that interference phenomena are rather sensitive to the small variations in the system.

Our experimental results were obtained for an optical system in which the polarization dynamics of the light can be described by a Schrödinger-like equation. The observed effects of geometric origin are to be expected also in, e.g., atomic and molecular collision experiments or in two-level atom (or spin-1/2) experiments in which a complex coupling

gives rise to a twist function. In the case of two-level atoms such a twist function can, for example, be realized by applying electromagnetic fields which are frequency modulated [11].

#### ACKNOWLEDGMENTS

This work is part of the research program of the Foundation for Fundamental Research on Matter (FOM) and was made possible by the financial support from the Netherlands Organization for Scientific Research (NWO).

- 
- [1] M. V. Berry, Proc. R. Soc. London Ser. A **392**, 45 (1984).  
 [2] A. Shapere and F. Wilczek, *Geometric Phases in Physics* (World Scientific, Singapore 1989).  
 [3] M. V. Berry, Proc. R. Soc. London Ser. A **430**, 405 (1990).  
 [4] K. Nakamura and S. A. Rice, Phys. Rev. A **49**, R2217 (1994); K. Nakamura, *Quantum Chaos*, Cambridge Nonlinear Science Series 3 (Cambridge University Press, Cambridge, 1993).  
 [5] A. Joye, G. Miletì, and Ch.-Ed. Pfister, Phys. Rev. A **44**, 4280 (1991); A. Joye, H. Kunz, and Ch.-Ed. Pfister, Ann. Phys. **208**, 299 (1991).  
 [6] J. W. Zwanziger, S. P. Rucker, and G. C. Chingas, Phys. Rev. A **43**, 3232 (1991).  
 [7] A. M. Dykhne, Zh. Éksp. Teor. Fiz. **41**, 1324 (1961) [Sov. Phys. JETP **14**, 941 (1962)]; J. P. Davis and P. Pechukas, J. Chem. Phys. **64**, 3129 (1976); J.-T. Hwang and P. Pechukas, *ibid.* **67**, 4640 (1977).  
 [8] The often stated criterion that only the branch points nearest to the real time axis are important is incorrect, as was pointed out in Ref. [5].  
 [9] R. J. C. Spreeuw and J. P. Woerdman, in *Progress in Optics*, edited by E. Wolf (North-Holland, Amsterdam, 1993), Vol. 31, pp. 263–319, and references therein; D. Bouwmeester, N. H. Dekker, F. E. v. Dorsselaer, C. A. Schrama, P. M. Visser, and J. P. Woerdman, Phys. Rev. A **51**, 646 (1995); C. A. Schrama, D. Bouwmeester, G. Nienhuis, and J. P. Woerdman, *ibid.* **51**, 641 (1995).  
 [10] R. Clark Jones, J. Opt. Soc. Am. **31**, 488 (1941).  
 [11] G. S. Agarwal and W. Harshawardhan, Phys. Rev. A **50**, R4465 (1994).